



# Thermal analysis of multi-layer walls containing geopolymer concrete and phase change materials for building applications

Vinh Duy Cao, Tri Quang Bui, Anna-Lena Kjøniksen\*

Faculty of Engineering, Østfold University College, P.O. Box 700, N-1757, Halden, Norway

## ARTICLE INFO

### Article history:

Received 18 February 2019

Received in revised form

4 July 2019

Accepted 19 July 2019

Available online 22 July 2019

### Keywords:

Microencapsulated phase change materials

Phase change materials

Geopolymer concrete

Energy efficiency

## ABSTRACT

A numerical model based on the finite differences method was developed to analyze the effect of seasonal variations, human comfort temperature, and wall design on the thermal performance of a single house dwelling in the climate conditions of Oslo (Norway) utilizing multilayer walls containing phase change materials. Special attention was given to the addition of an insulating layer and on variations of the assumed human comfort temperature, since these factors have received little attention previously. The thermal performance was found to be significantly improved by integrating microencapsulated phase change materials (MPCM) into geopolymer concrete and by adding pure phase change materials (PCM) to multilayer walls. Optimum conditions (thick PCM layer and thin insulating layer) resulted in an annual energy reduction of 28–30%. PCM was found to be more effective when it was located closer to the outdoor environment. Increasing the thickness and reducing the thermal conductivity of the insulation layer significantly decrease the energy consumption of a heating and cooling system, but reduces the effectiveness of the high heat storage capacity of the MPCM/PCM. The multilayer walls exhibited best performance in summer, with up to 32% energy reduction in the lower range of the considered human comfort zones (18 °C).

© 2019 The Authors. Published by Elsevier Ltd. This is an open access article under the CC BY-NC-ND license (<http://creativecommons.org/licenses/by-nc-nd/4.0/>).

## 1. Introduction

Phase change materials (PCM) are able to store and release large amounts of thermal energy during the phase change. Integration of PCMs in buildings [1–16] improve the thermal energy storage capacity, leading to reduced energy consumption. This is a promising solution for using less energy to maintain a comfortable indoor temperature. Considering that approximately 40% of the total energy consumption in cities is related to heat regulation of buildings [17,18], this can contribute to a considerable reduction of energy consumption. PCM can be incorporated into different parts of buildings such as walls, ceilings, windows, and floors. Of these, integration of PCM into walls have received special attention due to the larger exposed surface area. PCM can be sandwiched between the external and internal layers of multi-layer walls [19,20], or integrated into cements, mortars, concretes, and gypsum panels as microencapsulated phase change materials (MPCM) [7,11,12,21–25]. Both experimental and numerical studies illustrate

a very promising potential for saving energy by integrating PCM into walls [7,8,22]. Compared to experimental studies, which are usually costly and time consuming, simulations are able to determine the efficiency of a design without physically building the systems. This leads to reduced investigation times and the much lower overall cost.

Most previous studies are investigating the correlation between the PCM properties (phase change temperature, heat of fusion, PCM concentration, PCM thickness) and the outdoor environmental conditions (outdoor temperature, season, solar radiation) [19,21,26,27] on the energy efficiency of the buildings. However, studies on the effects of insulation and the presumed human comfort zone on the effectiveness of PCM in buildings are scarce, although these factors play an important role on the thermal performance. Furthermore, there are conflicting observations regarding the influence of season (summer, winter, spring and autumn) on the effectiveness of PCM in buildings [28–30]. Dissimilarities in the considered climate conditions (solar radiation, outdoor temperature variations), building design (wall structure, PCM type) and the human comfort zone applied in the models might be the cause for these discrepancies.

The present work describes a mathematical model based on the

\* Corresponding author.

E-mail address: [anna.l.kjoniksen@hiof.no](mailto:anna.l.kjoniksen@hiof.no) (A.-L. Kjøniksen).



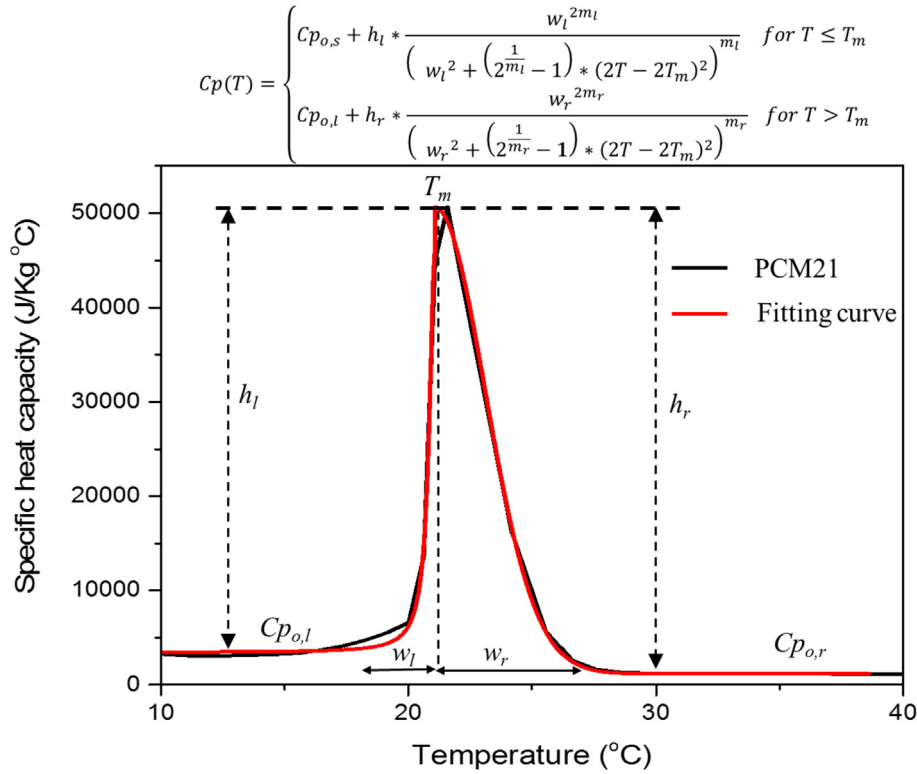


**Fig. 1.** The specific heat capacity of the phase change materials RT21 (PCM21) as a function of temperature. The black solid line is experimental values obtained by DSC. The red line shows the fitted values according to Eq. (1).

where  $T_m$ ,  $w_l$  and  $w_r$  are the melting temperature, and the phase change temperature range on the left side and right side of the melting peak, respectively.  $h_l$ ,  $h_r$ ,  $m_l$  and  $m_r$  are the height of the melting peak on the left and right side, and the shape parameters for the left and right side of the peak, respectively.  $C_{p_{o,s}}$  and  $C_{p_{o,l}}$  are respectively the specific heat capacity of solid PCM and liquid PCM (outside the melting range). See Cao et al. [23] for more information about the  $C_p(T)$  fitting process. The thermal properties of the materials used for the multi-layer walls are summarized in Table 2.

### 2.3. Numerical method

A passive single-family home with geopolymer concrete walls containing MPCM and a PCM layer was numerically evaluated at the climatic conditions of Oslo, Norway. The simulated home dimensions were generated according to Norwegian building standards TEK17, where the total wall area of a single-family home in Oslo is about  $132 \text{ m}^2$  [36]. Accordingly, the north and south walls were assumed to be  $3 \times 12 \text{ m}^2$ , while the east and west walls were set to  $3 \times 10 \text{ m}^2$ . All walls were made of multi-layers as illustrated in Fig. 2. The reference walls were made of three layers consisting of an insulation layer sandwiched between two pure geopolymer concrete walls (Fig. 2b). In order to investigate the influence of MPCM on the thermal performance, geopolymer concrete containing 5.2 wt% of MPCM was used to replace the pure geopolymer concrete. Furthermore, the effect of PCM on thermal performance of the house was also determined by adding a layer of pure PCM, as illustrated in Fig. 2c. This combination is denoted MPCM/PCM walls.

The following assumptions of the material properties and environmental conditions were made to simplify the calculation process:

- The thickness of the multi-layer walls is significantly smaller than the other dimensions. Therefore, the heat transfer process across the concrete walls is assumed as a one-dimensional problem.
- The wall layers are homogeneous and isotropic.
- There is no heat generation in the wall layers.
- The convection effect in the melted PCM is omitted.
- The heat from people and devices are neglected.
- The contact resistances between wall layers are neglected
- The ceiling and floor are assumed to be fully insulated, so that there is no heat gain/loss through them.
- The thermal exchange with the ground is neglected.

Under the above assumptions, for a wall facing the  $b$  direction (south, east, north and west), the local wall temperature  $T_j$  within layer  $j$  at any time  $t$  and location  $x$  is governed by the 1-D transient heat conduction equation given by Refs. [37–39]:

$$k_{j,b} \frac{\partial^2 T_{j,b}}{\partial x^2} = \rho_{j,b} C_{p_{j,b}}(T) \frac{\partial T_{j,b}}{\partial t} \quad 2$$

where  $k_{j,b}$ ,  $\rho_{j,b}$ ,  $x$  are, respectively, the thermal conductivity, density, and thickness of layer  $j$  of a wall facing direction  $b$ .  $C_{p_{j,b}}(T)$  is the specific heat capacity as a function of temperature of layer  $j$ .

In order to numerically solve Eq. (2), the fully implicit finite difference method (first order in time), which has good accuracy for large time steps will be employed [40]. According to this method, the medium will be discretized into a number of nodes, where  $\Delta x$  is the distance (thickness) between two adjacent nodes. The volume elements over the nodes, where the energy balance is applied, are formed to determine the temperatures at all nodes of the sample (Fig. 4) [23,40].

The heat capacity method for simulating phase change has

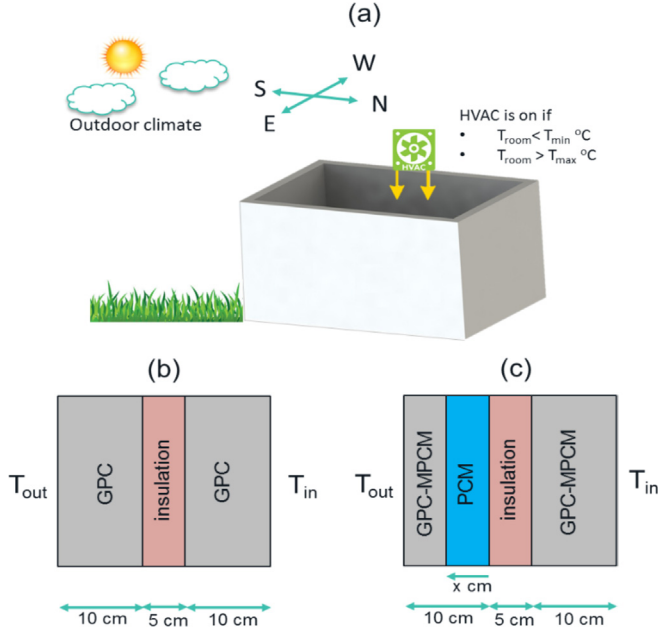


Fig. 2. (a) Illustration of a single house using multi-layer walls with (b) reference wall and (c) MPCM/PCM wall. It is assumed that the ceiling and floor is fully insulated.

previously been validated against experimental data [23].

- Interior node  $i = 1$  ( $x = 0$ , indoor wall surface) (boundary condition [37]): The wall was subjected to convective heat transfer at the inside surface

$$k_{1,b} \frac{T_{2,b}^{t+\Delta t} - T_{1,b}^{t+\Delta t}}{\Delta x_1} + h_i (T_{room}^{t+\Delta t} - T_{1,b}^{t+\Delta t}) = \rho_{1,b} C_{p1,b} \frac{\Delta x_1}{2} \frac{(T_{1,b}^{t+\Delta t} - T_{1,b}^t)}{\Delta t} \quad 3$$

- Inner node  $i$  in layer  $j$

$$k_{j,b} \frac{T_{i-1,b}^{t+\Delta t} - T_{i,b}^{t+\Delta t}}{\Delta x_j} + k_{j,b} \frac{T_{i+1,b}^{t+\Delta t} - T_{i,b}^{t+\Delta t}}{\Delta x_j} = \rho_{j,b} C_{pj,b} \Delta x_{j,b} \frac{T_{i,b}^{t+\Delta t} - T_{i,b}^t}{\Delta t} \quad 4$$

- Interface node between layer  $j$  and layer  $j+1$

$$k_{j,b} \frac{T_{i-1,b}^{t+\Delta t} - T_{i,b}^{t+\Delta t}}{\Delta x_j} + k_{j+1,b} \frac{T_{i+1,b}^{t+\Delta t} - T_{i,b}^{t+\Delta t}}{\Delta x_{j+1}} = \rho_{j,b} C_{pj,b} \frac{\Delta x_j}{2} \frac{T_{i,b}^{t+\Delta t} - T_{i,b}^t}{\Delta t} + \rho_{j+1,b} C_{pj+1,b} \frac{\Delta x_{j+1,b}}{2} \frac{T_{i,b}^{t+\Delta t} - T_{i,b}^t}{\Delta t} \quad 5$$

- Exterior node  $i = N$  ( $x = L$ , outdoor wall surface) (boundary condition [30,37,39,41]): the exterior wall surface is subjected to a real outdoor temperature and a solar radiation heat flux ( $q''_s$ ). The combined convective and radiative heat transfer is imposed at the exterior wall surface.

$$k_{n,b} \frac{T_{N-1,b}^{t+\Delta t} - T_{N,b}^{t+\Delta t}}{\Delta x_n} + h_o (T_{out}^{t+\Delta t} - T_{N,b}^{t+\Delta t}) + \alpha_s q''_{s,b} - \varepsilon \sigma \left( (T_{N,b}^{t+\Delta t})^4 - (T_{sky}^{t+\Delta t})^4 \right) = \rho_{n,b} C_{pn,b} \frac{\Delta x_n}{2} \frac{(T_{N,b}^{t+\Delta t} - T_{N,b}^t)}{\Delta t} \quad 6$$

$T_{i,b}^t$ ,  $T_{i,b}^{t+\Delta t}$  are the temperature of node  $i$  of the wall on direction  $b$  at time  $t$  and time  $(t+\Delta t)$ . In addition,  $\Delta t = 600$  s and  $\Delta x = 0.001$  m were selected for all cases in the current simulation. MATLAB (Mathworks Inc., Natick, MA, USA) was employed to program and solve the above equations for all nodes.

The Stefan-Boltzmann constant ( $\sigma$ ); the total absorptivity ( $\alpha_s$ ) and the emissivity ( $\varepsilon$ ) of the outdoor wall surface; the indoor heat transfer coefficient ( $h_i$ ) and the outdoor heat transfer coefficient ( $h_o$ ) were taken from ASHRAE [42]. Accordingly,  $h_i$  and  $h_o$  were respectively set to  $8 \text{ W/m}^2 \text{ K}$  and  $20 \text{ W/m}^2 \text{ K}$  [42], which has been utilized for similar calculations previously [39,43,44], while  $\alpha_s$  and  $\varepsilon$  were 0.65 and 0.87, respectively.

$T_{sky}$  and  $T_{N,b}$  are the average sky temperature and the outdoor wall surface temperature ( $x = L$ ). An average sky temperature  $T_{sky} = (T_{out} - 12) \text{ } ^\circ\text{C}$  was used [44,45]. The initial temperature was assumed uniform throughout the system and equal to  $20 \text{ } ^\circ\text{C}$ .

The outdoor temperature  $T_{out}$  and solar radiation  $q''_s$  as function of time for a typical year in Oslo for Eq. (2) were obtained from weather data and are shown in Fig. 5 and Fig. 6 (Climate Consultant software [46]).

The heat energy can be transferred from the wall to the room air by convection:

$$Q_{air} = \rho_{air} \times V_{air} \times C_{p-air} \times \frac{T_{room}^{t+\Delta t} - T_{room}^t}{\Delta t} = \sum A_b (q_{convection,b} + Q_{HVAC,b}) \quad 7$$

where  $A_b$  is the wall area in direction  $b$ ,  $q_{convection,b}$  and  $Q_{HVAC,b}$  are the unit energy convection (per  $1 \text{ m}^2$  wall area) and unit power consumption of the HVAC system of the  $b$  facing walls. The unit energy convection of each wall can be calculated as

$$q_{convection,b}(t) = h_{i,b} (T_{room}^t - T_{1,b}^t) \quad 8$$

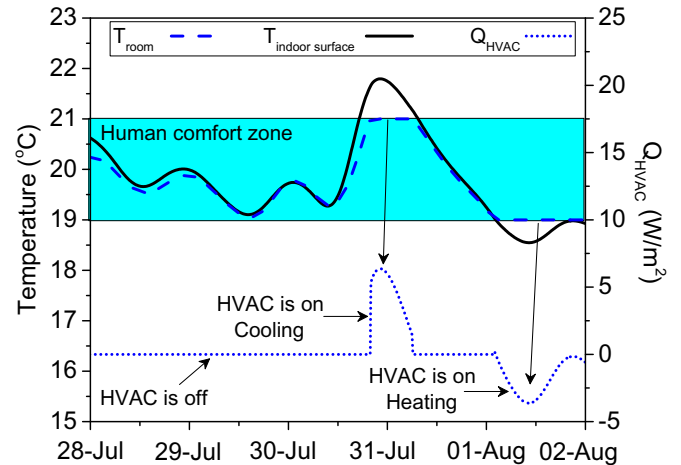


Fig. 3. The simulated indoor surface temperature, room temperature and compensated power from the HVAC system of a single house with MPCM/PCM walls.

The indoor temperature ( $T_{room}$ ) was controlled within the human comfort zone, with a temperature range of  $[T_{min} - T_{max}]$  by the heating and cooling system (HVAC). Accordingly, the HVAC will be on if the room temperature is outside the temperature range between  $T_{min}$  and  $T_{max}$ , to maintain the room temperature within the human comfort zone. The HVAC system will be off when  $T_{min} \leq T_{room} \leq T_{max}$ . The simulated compensated heating loss/gain through buildings by the HVAC system to maintain the room temperature within 19–21 °C is illustrated in Fig. 3. Accordingly, the power supplied by the HVAC system can be expressed as:

$$Q_{HVAC,b} = \begin{cases} q_{convection,b} & \text{if } T_{room} < T_{min} \text{ and } T_{room} > T_{max} \\ 0 & \text{if } T_{min} \leq T_{room} \leq T_{max} \end{cases} \quad 9$$

The energy consumption of the HVAC system for each wall orientation is equal to the heat loss/gain through the wall by convection:

$$E_b = \int_0^t |Q_{HVAC,b}| dt = \begin{cases} \int_0^t |q_{convection,b}| dt & \text{if } T_{room} < T_{min} \text{ and } T_{room} > T_{max} \\ 0 & \text{if } T_{min} \leq T_{room} \leq T_{max} \end{cases} \quad 10$$

The average energy consumption through all four wall orientations of a single house was also determined:

$$E_{ave} = \sum \frac{P_b}{4} \quad 11$$

The energy reduction  $E_r$  is:

$$E_r = \frac{E_{ave,ref} - E_{ave,MPCM/PCM}}{E_{ave,ref}} \cdot 100\% \quad 12$$

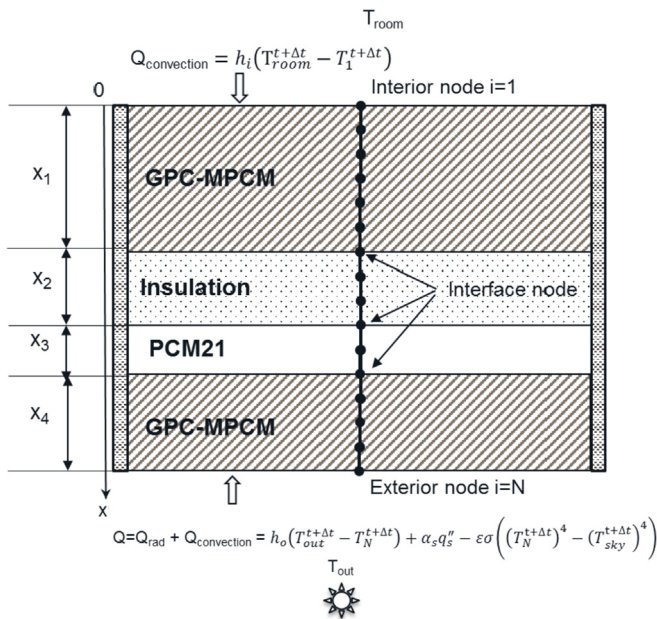


Fig. 4. Schematic representation of the multi-layer walls containing PCM materials with boundary conditions.

where  $E_{ave,ref}$  and  $E_{ave, MPCM/PCM}$  are the average energy consumption of the HVAC system for the reference wall and the MPCM/PCM wall, respectively.

### 2.3.1. Effect of MPCM addition and PCM layer

The thermal performance of walls containing geopolymer concrete with 5.2 wt% MPCM compared to walls containing pure geopolymer concrete was investigated. In order to improve the thermal performance of a family house, a thin layer of PCM was added and sandwiched between the insulation and concrete layers. In the simulations, the outer wall surfaces of the multi-layer walls were exposed to a realistic outdoor temperature variation and solar radiation while the indoor room temperature of the human comfort zone was kept in the range 19–21 °C. The thickness of the wall was kept constant at 25 cm with a 5 cm insulation layer, a 10 cm interior GPC-MPCM layer, and a (10-x) cm exterior GPC-MPCM layer. A PCM layer of x cm was sandwiched between the insulation layer and the exterior GPC-MPCM layer. x was varied from 0 to 5 cm. Further-

more, the effect of the PCM layer position on the thermal performance was also investigated.

### 2.3.2. Effect of insulation layer properties

The thickness of the insulation layer and its thermal conductivity were varied in order to evaluate the effect of insulation layer on the thermal performance of a single-family house. The insulation layer thickness was varied from 2.5 to 10 cm while its thermal conductivity was changed from 0.02 to 0.10 W/m °C. The energy reduction was determined by comparing with corresponding reference walls, which contain 10 cm GPC on each side and x cm (2.5–10 cm) of the insulation layer in the middle. The human comfort zone was set as 19–21 °C.

### 2.3.3. Effect of the human comfort zone

Since different people have dissimilar preferences regarding in

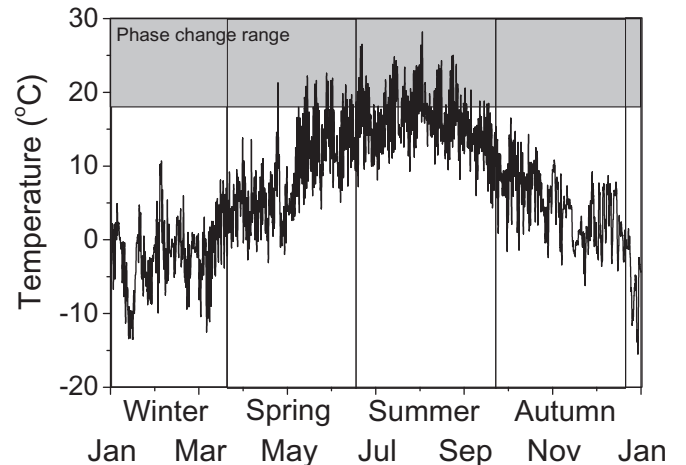


Fig. 5. The outdoor temperature (obtained from weather data-Climate Consultant software [46]) in Oslo.

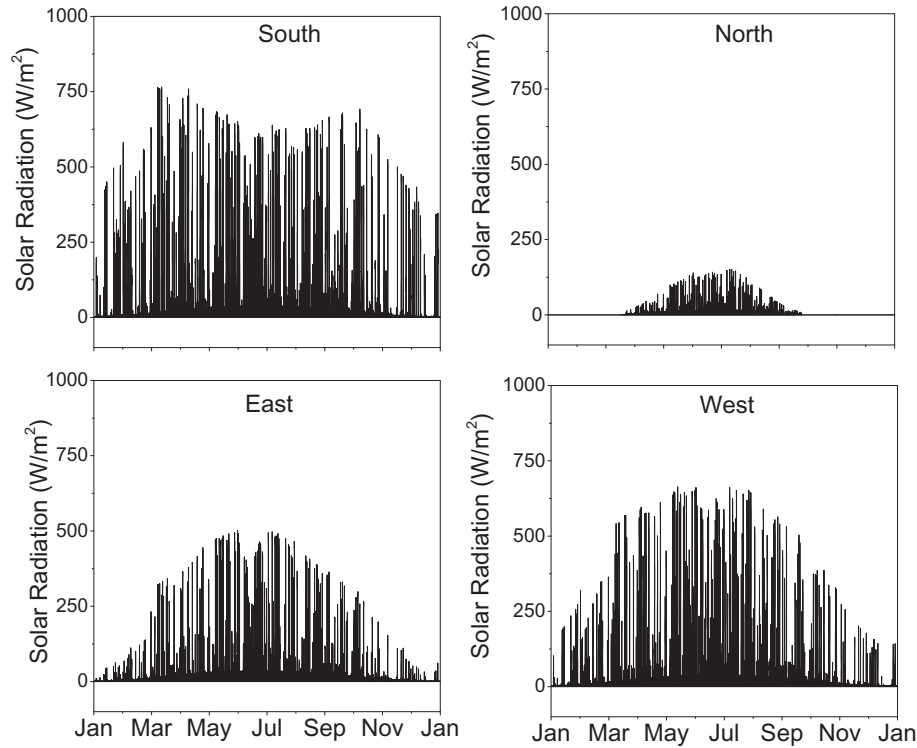


Fig. 6. The time-dependent solar radiation of different directions in Oslo (obtained from weather data-Climate Consultant software [46]).

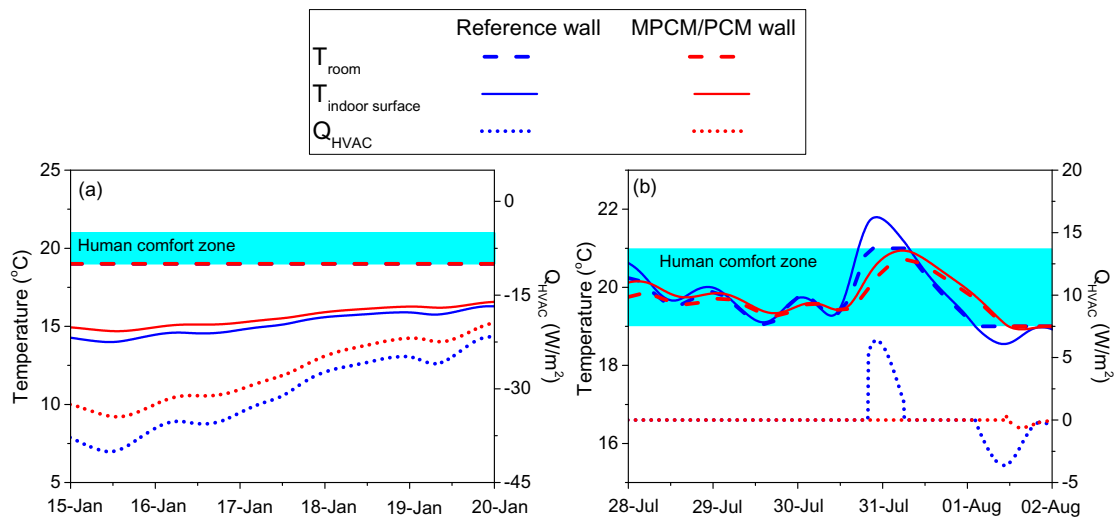


Fig. 7. The simulated indoor surface temperature, room temperature and compensated power from the HVAC system of a single house using a reference wall and MPCM/PCM walls during (a) 15th to 20th of January (winter) and (b) 28th of July to 02<sup>nd</sup> of August (summer).

which temperature range they feel comfortable, it is therefore interesting to evaluate how these preferences affect the energy consumption and energy reduction of the HVAC system. In these simulations, the thickness of the MPCM/PCM walls is 25 cm with a 5 cm insulation layer ( $k=0.10\text{ W/m }^\circ\text{C}$ ), and a 3 cm PCM layer at position 1 (closer to the outdoor environment). For the human comfort zone, the average maintained indoor temperature  $(T_{\max} + T_{\min})/2$  was varied from  $18^\circ\text{C}$  to  $25^\circ\text{C}$  (in steps of  $1^\circ\text{C}$ ) while the maintained indoor temperature amplitude  $(T_{\max}-T_{\min})/2$  was set to 1, 2, and  $3^\circ\text{C}$ . The utilized temperatures are similar to the human comfort zone recommended in ASHRAE [42] and in other previous calculations [21,26].

### 3. Results and discussions

#### 3.1. Effect of MPCM addition and PCM layer

The effect of utilizing a GPC-MPCM layer and a PCM layer was investigated. A schematic of the MPCM/PCM walls and the reference walls is depicted in Fig. 8. Fig. 7 shows the  $Q_{\text{HVAC}}$ , the indoor surface temperature and the room temperature as a function of time for a south-facing wall during winter (from 15th to 20th of January - Fig. 7a) and during summer (from 28th of July to 02<sup>nd</sup> of August - Fig. 7b) at the climate conditions of Oslo. The higher heat storage capacity and lower thermal conductivity (Table 2) of the

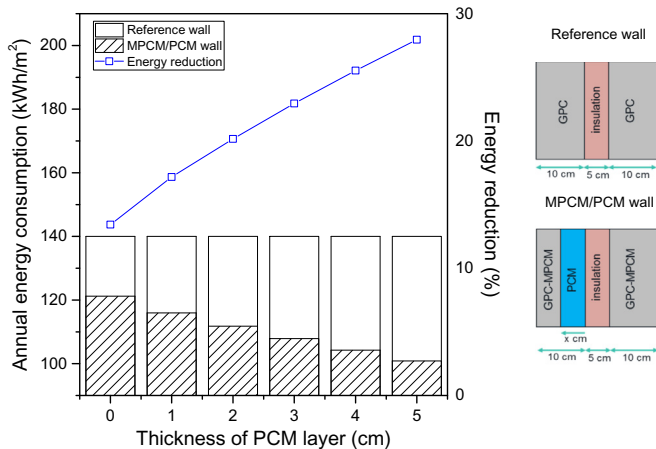


**Fig. 8.** The annual energy consumption and energy reduction of the HVAC system for maintaining the room temperature within the human comfort zone of 19–21 °C as function of PCM layer thickness. The inserted pictures illustrate the reference wall and the MPCM/PCM wall.

wall containing GPC-MPCM maintain the temperature better than the reference wall. Therefore, the HVAC system requires a lower amount of heating and cooling power. As can be seen from Fig. 7b, during these summer days utilization of GPC-MPCM maintains the room temperature within the human comfort zone without the need of a HVAC system.

The total energy consumption for the HVAC system is the sum of the heating energy consumption when the indoor surface temperature is in the range  $T_{i=1,x=0} < T_{room}$  (heating zone), and the cooling energy consumption when the indoor surface temperature is in the range  $T_{i=1,0} > T_{room}$  (cooling zone). The annual energy consumption for the HVAC system to keep the room temperature within the human comfort zone and the energy reduction due to the utilization of MPCM/PCM are calculated by Eq. (10)–(12) and are summarized in Fig. 8. After adding 5.2 wt% of MPCM, the annual energy consumption decreases from 140 kWh/m<sup>2</sup> (for the reference wall without MPCM) to 121 kWh/m<sup>2</sup> corresponding to a 13% energy reduction.

The addition of a PCM layer to the wall has a significant effect on the thermal performance of the single house. As can be seen in Fig. 8, the annual energy consumption of the HVAC system to maintain the room temperature within the human comfort zone (19–21 °C) decreases significantly when the thickness of the PCM layer increases. The annual energy reduction reach approximately 28% after adding a PCM layer of 5 cm. The higher PCM concentration in the wall when the thickness of the PCM layer is raised cause an increase of the overall thermal resistance and heat storage capacity of the wall. The annual energy savings in the current work (28%) is relatively high compared to previous studies (Chan- 3% in Hong Kong [47], Peippo et al. – 15% in Wisconsin (USA) [48], Thiele et al. – 18% in San Francisco (USA) and 32% in Los Angeles (USA) [49], Diaconu et al. – 12.8% in Béchar (Algeria) [30]). Although the configuration of the wall, the PCM materials and climate conditions are different between the current work and the previous studies, the better annual energy saving is a very promising result of the current work.

The thermal performance of two different positions of the PCM layer (Fig. 9) was also investigated. They are called position 1, where PCM layer is closer to outdoor environment, and position 2, where PCM layer is closer to indoor condition. The thickness of the wall was kept constant at 25 cm with a 5 cm insulation layer, and a 1–5 cm PCM layer.

The temperature variation across the PCM layer at different PCM

positions and the energy reduction compared to a corresponding reference wall during summer and winter are shown in Fig. 9. During summer, the temperature variation across the PCM layer is within the PCM melting temperature range for both cases. This utilizes the effect of the high heat storage capacity of PCM during the phase change. As can be seen from Fig. 9a, when the PCM layer is at position 2 (closer to the indoor environment) the temperature variations fluctuate less than at position 1 (closer to the outdoor environment). The lower temperature variation within the melting temperature range can minimize the effect of the phase change, causing a lower energy efficiency of the PCM layer [20]. Accordingly, the wall with the PCM layer at position 1 has a higher energy efficiency than at position 2. This observation is in good agreement with Fig. 9c, where the wall with the PCM layer at position 1 (closer to the outdoor environment) has a higher energy reduction compared to position 2 (closer to the indoor environment) during summer. However, there is no difference between two positions during winter (Fig. 9d). This is because the low outdoor temperature during winter keeps the temperature variations through the PCM layer below the melting temperature range of the PCM (Fig. 9b). Accordingly, the effect of the high heat storage capacity during phase change is not utilized at these conditions. This observation is consistent with previous studies [21,28,47,49], where the energy efficiency of the walls containing a PCM/MPCM in Madrid and Oslo [21], Hongkong [47], Miami [28], San Francisco and Los Angeles [49] were numerically investigated. As in the previous studies, the energy efficiency of the walls containing PCM/MPCM can be maximized in climates where the outdoor temperature varies around the phase change temperature range. As can be seen in Fig. 9c and d, increasing the thickness of the PCM layer causes a higher energy reduction. This is expected both since the heat storage capacity is enhanced by the higher PCM content, and because the PCM layer has a lower thermal conductivity than the concrete layer, thereby providing better insulating properties. However, the thickness of the PCM layer does not affect the influence the placement of the PCM layer has on the energy reduction.

### 3.2. Effect of the insulation layer

The effect of the insulation layer thickness was investigated utilizing the dimension of the walls as illustrated in Fig. 10. As can be seen from Fig. 10, there is a decline in the annual energy consumption when the thickness of the insulation layer is increased for both the reference and MPCM/PCM walls. This is expected because the heat transfer through the wall is inversely proportional to the wall thickness, thereby reducing the heat loss or gain, leading to a decline in energy consumption for maintaining the indoor temperature [21]. However, a thicker insulation layer causes lower reduction of energy consumption as shown in Fig. 10. This is due to both the reduced energy consumption and the reduced heat transfer rate in the presence of a thick insulating layer. This demonstrates that the energy efficiency of MPCM and PCM addition is decreased when the thickness of the insulation layer is raised. Another drawback of a thicker insulation layer is very thick walls resulting in a reduction of useable housing area.

The thermal conductivity of the insulation layer was varied from 0.02 to 0.10 W/m °C in order to evaluate the effect on the energy efficiency of the walls. In this test, the thickness of the wall was kept constant at 25 cm with a 5 cm insulation layer. Fig. 11 shows the effect of the thermal conductivity of the insulation layer on the annual energy consumption and energy reduction of a single house at the climate conditions of Oslo. As expected, the energy consumption for maintaining the indoor temperature within the human comfort zone decreases significantly when the thermal conductivity of the insulation layer is reduced. Accordingly, the

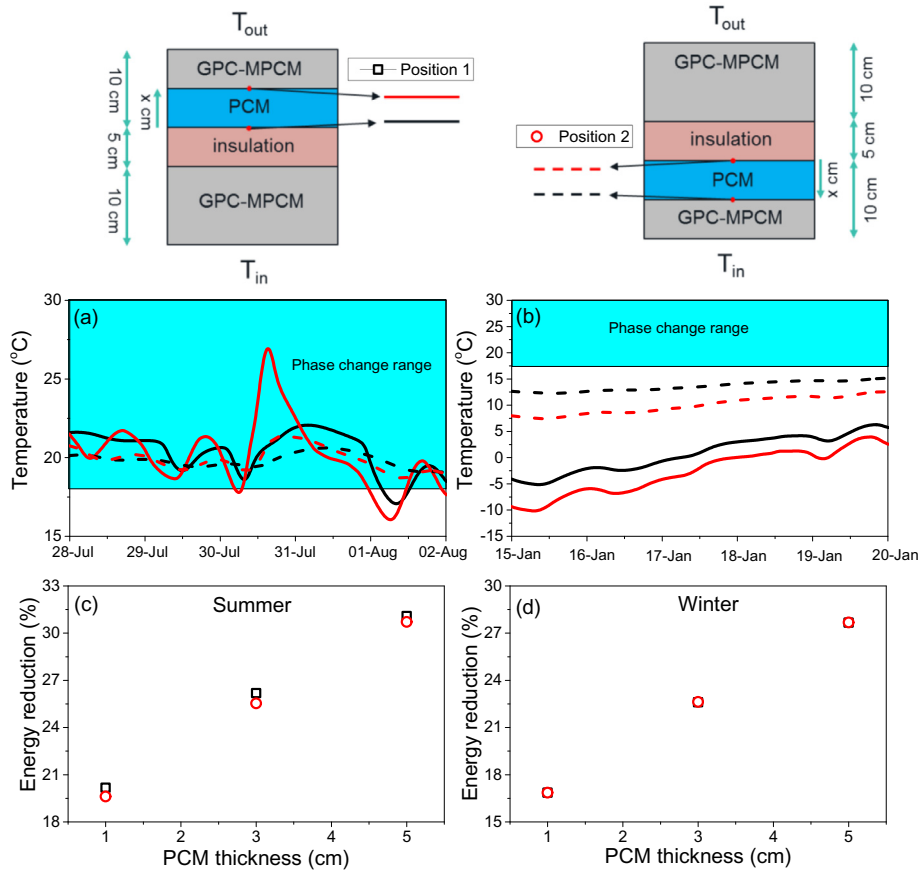


**Fig. 9.** The temperature variation across PCM layer during (a) 28th July to 02<sup>nd</sup> August (summer) and (b) 15th January to 20th January (winter); energy reduction of the HVAC system as function of PCM thickness during (c) summer and (d) winter at different positions of the PCM layer in the MPCM/PCM walls. The inserted pictures illustrate the different PCM layer positions in the MPCM/PCM walls.

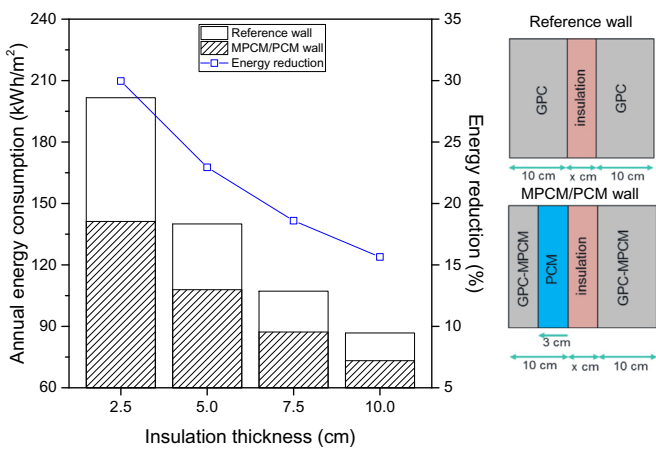


**Fig. 10.** The annual energy consumption and energy reduction of the HVAC system for a single house utilizing a reference wall and a MPCM/PCM wall as a function of the insulation thickness. The inserted pictures depict the reference wall and the MPCM/PCM wall.

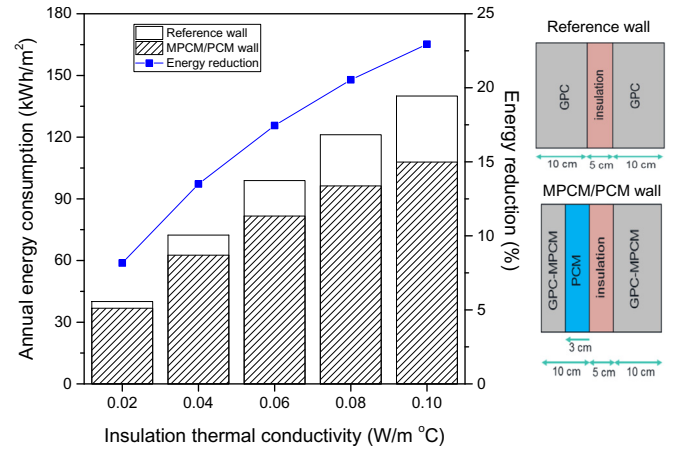


**Fig. 11.** The annual energy consumption of a HVAC system to maintain an indoor temperature within 19–21 °C of a single house utilizing reference and MPCM/PCM walls, and the energy reduction when utilizing MPCM/PCM walls. The inserted pictures illustrate the reference and MPCM/PCM walls.

energy consumption utilizing the MPCM/PCM walls decreases from 108 kWh/m<sup>2</sup> ( $k = 0.10$  W/m °C) to approximately 37 kWh/m<sup>2</sup> ( $k = 0.02$  W/m °C). However, the lower thermal conductivity of the insulation layer results in a lower energy efficiency of MPCM and PCM addition. When the thermal conductivity of the insulation layer decreases from 0.10 to 0.02 W/m °C, the energy reduction is

dramatically reduced from 23% to 8%.

The energy efficiency of PCM addition is strongly depended on the capacity of storing or releasing heat during phase change and on the outdoor and indoor temperature [19,21,26]. Typically, in building applications the PCM should go through a complete phase transition during a day in order to be fully effective. In the current

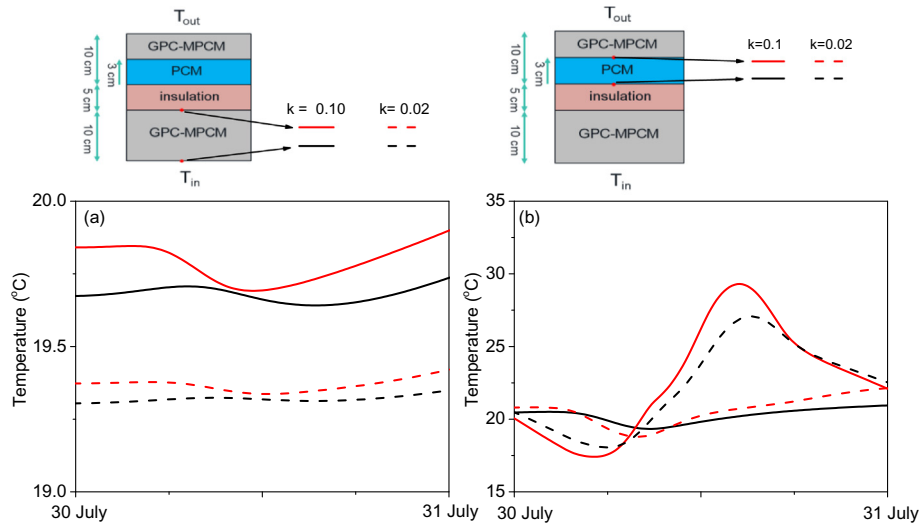


**Fig. 12.** The temperature variation across (a) the GPC-MPCM layer and (b) the PCM layer during 30th – 31st of July. The inserted pictures are the MPCM/PCM walls. Effect of the human comfort zone.

walls, both the overall thermal conductivity and the heat storage capacity have a strong effect on the heat transfer of the materials and the energy consumption of the HVAC system. They also have a relative effect on each other. The thermal conductivity is a parameter which is used to characterize the ability of a material to transmit heat, while the heat storage capacity is the ability of materials to store or release thermal energy. At a low thermal conductivity, it is difficult to transfer the heat to the indoor environment from the outdoor environment, leading to reduced

temperature variations across the walls. In this case, the effect of the heat storage capacity of the PCM on the heat transfer process across the wall is limited when the temperature variation within the PCM is too small. Consequently, the effect of the heat storage capacity on the energy performance is neglectable while the thermal conductivity is the dominant effect for stabilizing the interior temperature. This conjecture is strengthened by Fig. 12, where the temperature variation across the PCM layer and inner GPC-MPCM layer during 30th and 31st of July is within the phase change

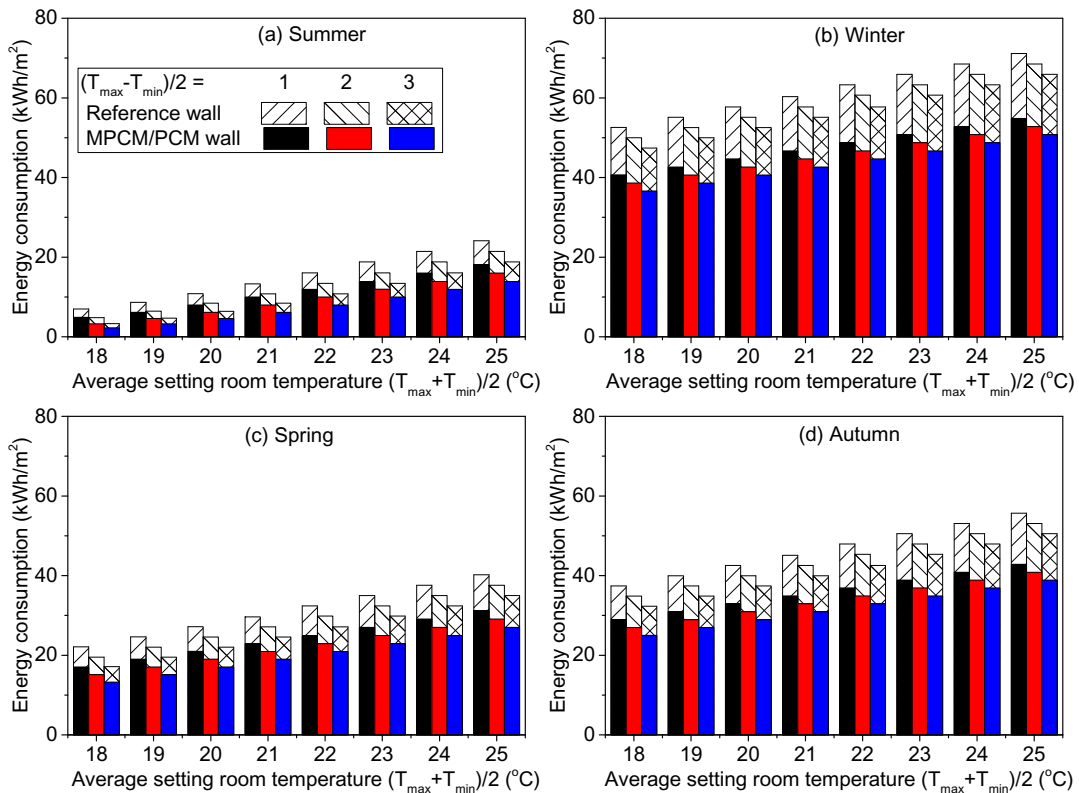


**Fig. 13.** The effect of the human comfort zone temperature on the energy consumption of a HVAC system in (a) summer, (b) winter, (c) spring and (d) autumn at the climate conditions of Oslo.

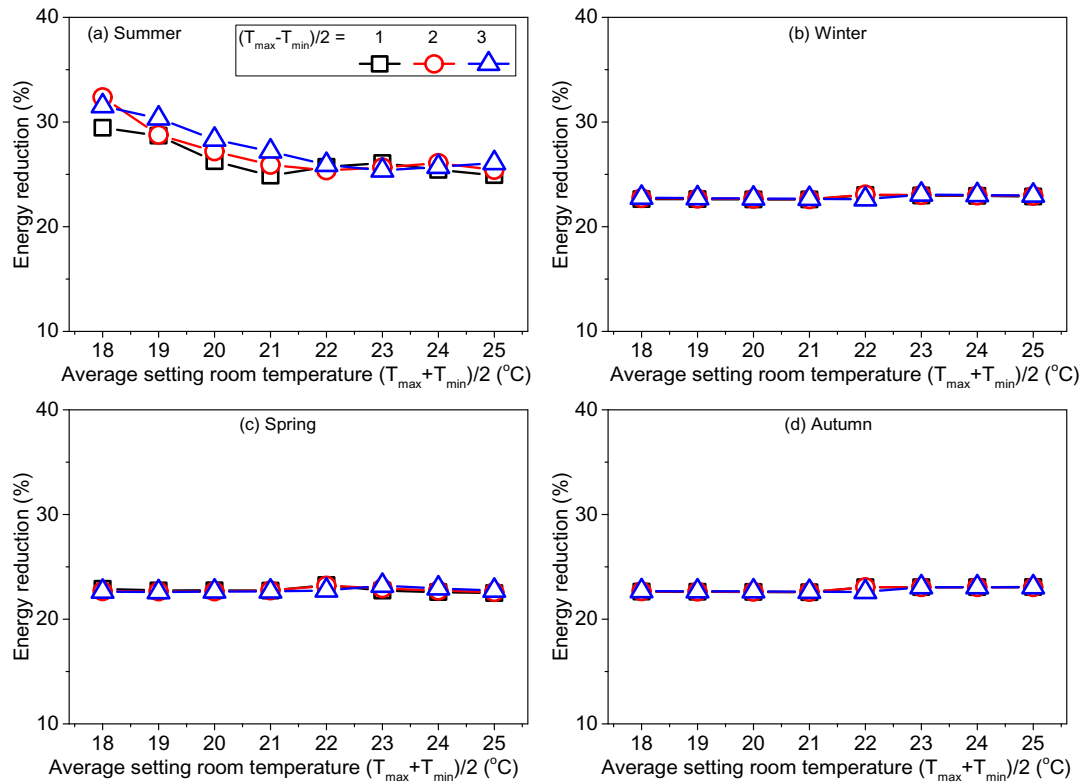


Fig. 14. The effect of the human comfort zone temperature on the energy reduction in (a) summer, (b) winter, (c) spring and (d) autumn at the climate conditions of Oslo.

temperature range, and is significantly decreased after reducing the thermal conductivity of the insulation layer from 0.10 W/m °C to 0.02 W/m °C. Furthermore, the low average outdoor temperature of Oslo also contributes to reducing the effectiveness of PCM addition when the thermal conductivity of the insulation layer is reduced.

Since people often disagree about what is a comfortable indoor temperature, it is interesting to examine the effect of the considered human comfort zone. In order to determine the effect of the human comfort zone on the thermal performance of a single house utilizing MPCM/PCM walls, the relationship between various indoor temperature ranges and the energy efficiency was studied. The energy consumption and energy reduction as a function of the average maintained indoor temperature are presented in Fig. 13 and Fig. 14, respectively.

Fig. 13 shows that the energy consumption increases when the

average maintained indoor temperature is raised and decreases when the maintained indoor temperature variation becomes higher for both the reference and MPCM/PCM walls. This is in agreement with Fig. 15b where the compensated power from the HVAC system ( $Q_{HVAC}$ ) during 24th July to 08th August increases significantly when the average setting of the indoor temperature is raised. The energy consumption is lowest during summer and highest during winter. This is caused by an outdoor temperature variation during the summer months (Fig. 5) which is within the phase change temperature range. In addition, the phase change temperature range and the maintained indoor temperature overlap, leading to an improvement of the effect of the high latent heat of the PCM, and a reduction of the heat loss/gain through the walls. During winter, the low outdoor temperature compared to the maintained indoor temperature (Fig. 5) will increase the heat loss

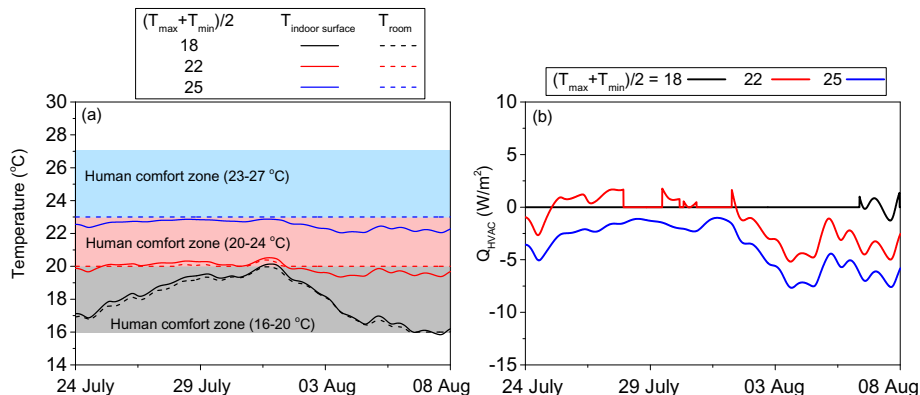


Fig. 15. (a) The indoor surface temperature and the room temperature; and (b) the compensated power from the HVAC system ( $Q_{HVAC}$ ) at an average setting of the room temperature  $(T_{max} + T_{min})/2$  of 18 °C, 22 °C and 25 °C. The setting room temperature amplitude  $(T_{max} - T_{min})/2$  is 2 °C.

from the house and extinguish the effect of the high latent heat during the phase change. This can also explain why the energy reduction is highest during summer and lowest in winter (Fig. 14). In addition, the lower energy consumption and higher energy reduction in summer compared to the other seasons reveals that the utilized MPCM/PCM is more effective in warmer climates. Interestingly, the energy reduction of the MPCM/PCM walls decreases from 33% to 26% when the average indoor temperature is increased from 18 °C to 22 °C, and reaches a plateau (around 26%) at higher maintained indoor temperatures during summer. On the other hand, the energy reduction is independent on the average indoor temperature for the rest of the year (about 22–23%). The energy reduction when utilizing MPCM/PCM walls is strongly dependent on the high heat storage capacity during the phase change [19]. Since the phase change transition is only properly utilized during summer (Figs. 7 and 9), the maintained indoor temperature has little effect on the energy reduction during the other seasons. In addition, the effectiveness of PCM addition decreases when the average maintained indoor temperature is raised during in the summer months. This observation can be explained by Fig. 15, which presents the indoor surface temperature and room temperature at different average settings of the indoor temperature (18 °C, 22 °C and 25 °C) and the corresponding compensated power from the HVAC system of a single house from 24th July to 08th August. As can be seen from Fig. 15a, the indoor surface temperature variations are mostly within the setting temperature range for the lowest range (16–20 °C), and accordingly the HVAC system is barely in use (Fig. 15b). At the higher indoor setting temperature ranges, the indoor surface temperature is lower than the range for extended periods of time, causing a higher energy consumption. The annual total cooling and heating loads were reduced by up to 1% and 13%, respectively, when the phase change temperature of PCM within the outer and inner layers was near the desired indoor temperature. However, this contradicts previous studies [15–17] where the cooling energy savings were reported to be larger than the heating energy savings. This discrepancy is probably due to climate conditions in Algeria that resulted in a unidirectional wall heat flux during a large portion of the summer but not during the winter.

#### 4. Conclusion

A numerical model based on the finite differences method was developed to predict the thermal performance of a single house utilizing multi-layer walls containing phase change materials (layers of geopolymer concrete containing MPCM and a PCM layer) at the climate conditions of Oslo, Norway. Application of this numerical model is much faster and cheaper than experimental studies, and can therefore be of great help when designing energy efficient building envelopes. The addition of geopolymer concrete containing MPCM layers and a PCM layer to the multi-layer walls was found to significantly reduce the energy consumption of buildings. The annual energy reduction when utilizing walls containing 15 cm GPC-MPCM (5.2 wt%), a 5 cm PCM layer and a 5 cm insulation was approximately 28% compared to the reference when the maintained indoor temperature was 19–21 °C. The PCM layer was more effective when it was placed closer to the outdoor environment. Furthermore, the insulation layer has a significant impact on the thermal performance of these multi-layer walls. Although an increased thickness and a reduction of the thermal conductivity of the insulation layer reduce the energy consumption, it also diminishes the effectiveness of the high heat storage capacity of the MPCM/PCM layers. The thermal performance was found to be dependent on the season and the considered human comfort temperature. The energy consumption was lowest during

summer and highest during winter, while the energy reduction was highest during summer (up to 32%) and lowest during winter (about 23%). Interestingly, the energy efficiency of MPCM/PCM walls is strongly dependent on the considered human comfort zone in the summer months while it is independent of the indoor temperature for the rest of the year. The results illustrate that the developed model can be used as a quantitative tool to determine an optimal design of multi-layer walls containing MPCM/PCM in order to improve the thermal performance of buildings. The wall design (thickness, materials selection, phase change range of the PCM) should be carefully chosen taking into consideration the relevant climate conditions and the human comfort zone to obtain optimal energy efficient buildings.

#### Conflict of interest

The authors declare that we have no conflict of interest with respect to this paper.

#### Acknowledgement

We gratefully acknowledge funding from the Research Council of Norway, project number 238198.

#### References

- [1] Shadnia R, Zhang L, Li P. Experimental study of geopolymer mortar with incorporated PCM. *Constr Build Mater* 2015;84:95–102.
- [2] Borreguero AM, Serrano A, Garrido I, Rodríguez JF, Carmona M. Polymeric-SiO<sub>2</sub>-PCMs for improving the thermal properties of gypsum applied in energy efficient buildings. *Energy Convers Manag* 2014;87:138–44.
- [3] Eddhahak-Ouni A, Drissi S, Colin J, Neji J, Care S. Experimental and multi-scale analysis of the thermal properties of Portland cement concretes embedded with microencapsulated Phase Change Materials (PCMs). *Appl Therm Eng* 2014;64(1–2):32–9.
- [4] Pisello AL, D'Alessandro A, Fabiani C, Fiorelli AP, Ubertini F, Cabeza L F, Materazzi AL, FrancoCotana. Multifunctional analysis of innovative PCM-filled concretes. *Energy Procedia* 2017;111:81–90.
- [5] Wei Z, Falzone G, Wang B, Thiele A, Puerta-Falla G, Pilon L, Neithalath N, Sant G. The durability of cementitious composites containing micro-encapsulated phase change materials. *Cement Concr Compos* 2017;81:66–76.
- [6] Pilehvar S, Cao VD, Szczotok AM, Valentini L, Salvioni D, Magistri M, Pamies R, Kjøniksen A-L. Mechanical properties and microscale changes of geopolymer concrete and Portland cement concrete containing micro-encapsulated phase change materials. *Cement Concr Res* 2017;100.
- [7] Cao VD, Pilehvar S, Salas-Bringas C, Szczotok AM, Rodriguez JF, Carmona M, Al-Manasir N, Kjøniksen A-L. Microencapsulated phase change materials for enhancing the thermal performance of Portland cement concrete and geopolymer concrete for passive building applications. *Energy Convers Manag* 2017;133:56–66.
- [8] Hunger AGE M, Mandilaras I, Brouwers HJH, Founti M. The behavior of self-compacting concrete containing micro-encapsulated phase change materials. *Cement Concr Compos* 2009;31:731–43.
- [9] Cui H, Feng T, Yang H, Bao X, Tang W, Fu J. Experimental study of carbon fiber reinforced alkali-activated slag composites with micro-encapsulated PCM for energy storage. *Constr Build Mater* 2018;161:442–51.
- [10] Ramakrishnan S, Wang X, Sanjayan J, Petinakis E, Wilson J. Development of thermal energy storage cementitious composites (TESC) containing a novel paraffin/hydrophobic expanded perlite composite phase change material. *Sol Energy* 2017;158:626–35.
- [11] Ramakrishnan S, Wang X, Sanjayan J, Wilson J. Thermal energy storage enhancement of lightweight cement mortars with the application of phase change materials. *Procedia Eng* 2017;180:1170–7.
- [12] Ramakrishnan S, Wang X, Sanjayan J, Wilson J. Assessing the feasibility of integrating form-stable phase change material composites with cementitious composites and prevention of PCM leakage. *Mater Lett* 2017;192:88–91.
- [13] Cao VD, Pilehvar S, Salas-Bringas C, Szczotok AM, Do NBD, Le HT, Carmona M, Rodriguez JF, Kjøniksen A-L. Influence of microcapsule size and shell polarity on the TimeDependent viscosity of geopolymer paste. *Ind Eng Chem Res* 2018;57:9457–64.
- [14] Drissi S, Ling T-C. Thermal and durability performances of mortar and concrete containing phase change materials. *IOP Conf Ser Mater Sci Eng.* p. 062001.
- [15] Mazzeo D, Oliveti G. Thermal field and heat storage in a cyclic phase change process caused by several moving melting and solidification interfaces in the layer. *Int J Therm Sci* 2018;129:462–88.
- [16] Mazzeo D, Oliveti G, Arcuri N. Definition of a new set of parameters for the

- dynamic thermal characterization of PCM layers in the presence of one or more liquid-solid interfaces. *Energy Build* 2017;141:379–96.
- [17] EU Directive 2002/91/EC EP. Brussels. 2003.
- [18] EU Directive 2010/31/UE EP. Strasburg. 2010.
- [19] Wang Q, Wu R, Wu Y, Zhao CY. Parametric analysis of using PCM walls for heating loads reduction. *Energy Build* 2018;172:328–36.
- [20] Fateh A, Klinker F, Brütting M, Weinsläder H, Francesco Devia. Numerical and experimental investigation of an insulation layer with phase change materials (PCMs). *Energy Build* 2017;153:231–40.
- [21] Cao VD, Pilehvar S, Salas-Bringas C, Szczotok AM, Bui TQ, Carmona M, Rodriguez JF, Kjøniksen A-L. Thermal analysis of geopolymer concrete walls containing microencapsulated phase change materials for building applications. *Sol Energy* 2019;178:295–307.
- [22] Cao VD, Pilehvar S, Salas-Bringas C, Szczotok AM, Valentini L, Carmona M, Rodriguez JF, Kjøniksen A-L. Influence of microcapsule size and shell polarity on thermal and mechanical properties of thermoregulating geopolymer concrete for passive building applications. *Energy Convers Manag* 2018;164:198–209.
- [23] Cao VD, Pilehvar S, Salas-Bringas C, Szczotok AM, Bui TQ, Carmona M, Rodriguez JF, Kjøniksen A-L. Thermal performance and numerical simulation of geopolymer concrete containing different types of thermoregulating materials for passive building applications. *Energy Build* 2018;173:678–88.
- [24] Ramakrishnan S, Wang X, Sanjayan J, Wilson J. Thermal performance assessment of phase change material integrated cementitious composites in buildings: experimental and numerical approach. *Appl Energy* 2017;207:654–64.
- [25] Borreguero AM, Garrido I, Valverde JL, Rodríguez JF, Carmona M. Development of smart gypsum composites by incorporating thermoregulating microcapsules. *Energy Build* 2014;76:631–9.
- [26] Thiele AM, Liggett RS, Sant G, Pilon L. Simple thermal evaluation of building envelopes containing phase change materials using a modified admittance method energy buildings. 2017. p. 145.
- [27] Ramakrishnan S, Wang X, Sanjayan J, Wilson J. Thermal performance of buildings integrated with phase change materials to reduce heat stress risks during extreme heatwave events. *Appl Energy* 2017;194:410–21.
- [28] Zwanzig SD, Lian Y, Brehob EG. Numerical simulation of phase change material composite wallboard in a multi-layered building envelope. *Energy Convers Manag* 2013;69:27–40.
- [29] Biswas K, Abhari R. Low-cost phase change material as an energy storage medium in building envelopes: experimental and numerical analyses energy. *Convers Manage* 2014;88:1020–31.
- [30] Diaconu BM, Crueru M. Novel concept of composite phase change material wall system for year-round thermal energy savings. *Energy Build* 2010;42:1759–72.
- [31] Duxson P, Fernandez-Jimenez A, Provis JL, Lukey GC, Palomo A, Deventer JSJv. Geopolymer technology: the current state of the art. *J Mater Sci* 2007;42:2917–33.
- [32] Zuhua Z, Xiao Y, Huajun Z, Yue C. Role of water in the synthesis of calcined kaolin-based geopolymer. *Appl Clay Sci* 2009;43:218–23.
- [33] Davidovits J. Geopolymer chemistry and application. France: Institut Géopolymère; 2015.
- [34] Rajini B, Rao AVN. Mechanical properties of geopolymer concrete with fly ash and GGBC as source materials. *Int J Innov Res Sci Eng Technol* 2014;3:15944–53.
- [35] [https://www.rubitherm.eu/media/products/datasheets/Techdata\\_RT21\\_EN\\_05112015.PDF](https://www.rubitherm.eu/media/products/datasheets/Techdata_RT21_EN_05112015.PDF) Datasheet of RT21.
- [36] Kommunal og regionaldepartementet- Byggeteknisk forskrift TEK17. 2017.
- [37] Cengel YA. Heat transfer: a practical approach. second ed. McGraw-Hill; 2002.
- [38] Lamberg P, Lehtiniemi R, Henell A-M. Numerical and experimental investigation of melting and freezing processes in phase change material storage. *Int J Therm Sci* 2004;43:277–87.
- [39] Thiele AM, Sant G, Pilon L. Diurnal thermal analysis of microencapsulated PCM-concrete composite walls. *Energy Convers Manag* 2015;93:215–27.
- [40] Özişik MN, Orlande HRB, Colaço MJ, Cotta RM. Finite difference methods in heat transfer. Taylor & Francis Group; 2017.
- [41] Pasupathy LA A, Velraj R, Seeniraj RV. Experimental investigation and numerical simulation analysis on the thermal performance of a building roof incorporating phase change material (PCM) for thermal management. *Appl Therm Eng* 2008;28:556–65.
- [42] ASHRAE. Handbook of fundamentals. Atlanta: American Society of Heating, Refrigerating and Air-Conditioning Engineers; Inc.; 2013.
- [43] Alawadhi EM. Thermal analysis of a building brick containing phase change material. *Energy Build* 2008;40(3):351–7.
- [44] Al-Sanea SA. Thermal performance of building roof elements. *Build Environ* 2002;37:665–75.
- [45] Garg HP. Treatise on solar energy: fundamentals of solar energy. Chichester: Wiley; 1982.
- [46] [Energy-design-tools.aud.ucla.edu](http://energy-design-tools.aud.ucla.edu). UEDTGCCWh.
- [47] Chan ALS. Energy and environmental performance of building façades integrated with phase change material in subtropical Hong Kong. *Energy Build* 2011;43:2947–55.
- [48] Peippo K, Kauranen P, Lund PD. A multicomponent PCM wall optimized for passive solar heating. *Energy Build* 1991;17:259–70.
- [49] Thiele AM, Jamet A, Sant G, Pilon L. Annual energy analysis of concrete containing phase change materials for building envelopes. *Energy Convers Manag* 2015;103:374–86.